Peroxiredoxin 6 is required for blood vessel integrity in wounded skin

Angelika Kümin,[1] Matthias Schäfer,[1] Nikolas Epp,[1] Philippe Bugnon,[1] Christiane Born-Berclaz,[1] Annette Oxenius,[2] Anke Klippel,[3] Wilhelm Bloch,[4] and Sabine Werner[1]

[1]Institute of Cell Biology and [2]Institute of Microbiology, Department of Biology, ETH Zurich, Honggerberg, CH-8093 Zurich, Switzerland
[3]Atugen AG, 13125 Berlin, Germany
[4]Department of Molecular and Cellular Sport Medicine, German Sport University Cologne, 50927 Cologne, Germany

Peroxiredoxin 6 (Prdx6) is a cytoprotective enzyme with largely unknown in vivo functions. Here, we use Prdx6 knockout mice to determine its role in UV protection and wound healing. UV-mediated keratinocyte apoptosis is enhanced in Prdx6-deficient mice. Upon skin injury, we observe a severe hemorrhage in the granulation tissue of knockout animals, which correlates with the extent of oxidative stress. At the ultrastructural level endothelial cells appear highly damaged, and their rate of apoptosis is enhanced. Knock-down of Prdx6 in cultured endothelial cells also increases their susceptibility to oxidative stress, thus confirming the sensitivity of this cell type to loss of Prdx6. Wound healing studies in bone marrow chimeric mice demonstrate that Prdx6-deficient inflammatory and endothelial cells contribute to the hemorrhage phenotype. These results provide insight into the cross-talk between hematopoietic and resident cells at the wound site and the role of reactive oxygen species in this interplay.

Introduction

A large percentage of the population, in particular numerous aged individuals, patients with diabetes or cancer, or people treated with anti-inflammatory steroids, suffer from chronic, nonhealing wounds (Clark, 1996; Martin, 1997). Therefore, there is a strong need to develop strategies for the improvement of the repair process. This requires a thorough understanding of the underlying molecular and cellular mechanisms. A powerful approach to reach this goal is the identification and functional characterization of genes, which are regulated by skin injury and which are therefore candidate regulators of the repair process. Because the gene expression profile of the most malignant tumors resembles the profile of healing skin wounds (Chang et al., 2004), wound-regulated genes may also be important targets for the development of novel and efficient therapeutics for the treatment of cancer. Therefore, we used differential display RT-PCR and microarray analysis to identify genes that are regulated by skin injury in mice (Munz et al., 1999; Thorey et al., 2001). Interestingly, many of the identified injury-regulated genes encode enzymes, which detoxify reactive oxygen species (ROS), or transcription factors, which regulate these genes (Munz et al., 1997; Steiling et al., 1999; Hanselmann et al., 2001; Braun et al., 2002; auf dem Keller, 2006). Because large amounts of ROS are produced in early skin wounds by invading inflammatory cells as a defense against bacterial infection (Darr and Fridovich, 1994; Clark, 1996), the expression of ROS-detoxifying enzymes by cells in the wound tissue may be an important mechanism to protect inflammatory and resident cells from ROS toxicity.

One of the wound-regulated genes encodes peroxiredoxin 6 (Prdx6). Peroxiredoxins comprise a family of six enzymes that catalyze the reduction of hydrogen peroxide and a broad spectrum of organic peroxides. Prdx1–5 have two reactive cysteines and they use thioredoxin and/or glutathione as a substrate (Rhee et al., 2001; Fujii and Ikeda, 2002; Wood et al., 2003). By contrast, Prdx6—also designated 1-Cys-peroxiredoxin—has only a single redox-active cysteine (Manevich and Fisher, 2005). This cytosolic enzyme was reported to use glutathione (Manevich et al., 2004) or ascorbate (Monteiro et al., 2007) as reducing agent. In addition, Prdx6 displays phospholipase A_2 activity (Chen et al., 2000).

Recent studies revealed an important function of Prdx6 in the cellular stress response. Thus, overexpression of Prdx6 in different cell types protected from ROS-induced cytotoxicity

M. Schäfer and N. Epp contributed equally to this paper.

Correspondence to Sabine Werner: sabine.werner@cell.biol.ethz.ch

A. Klippel's present address is Wyeth Research, Department of Oncology Discovery, Pearl River, NY 10965.

Abbreviations used in this paper: GO, glucose oxidase; H/E, hematoxylin/eosin; HUVEC: human umbilical vein endothelial cells; Prdx, peroxiredoxin; ROS, reactive oxygen species; SMA, smooth muscle actin; UV, ultraviolet.

The online version of this article contains supplemental material.

The Journal of Cell Biology, Vol. 179, No. 4, November 19, 2007 747–760
http://www.jcb.org/cgi/doi/10.1083/jcb.200706090

(Manevich et al., 2002; Wang et al., 2004b), whereas antisense-mediated knockdown of this enzyme enhanced the sensitivity to oxidative stress (Pak et al., 2002; Mo et al., 2003; Wang et al., 2003). Prdx6 knockout mice were more sensitive to systemic treatment with the oxidative stress-inducing agent paraquat (Wang et al., 2003). They also showed increased lung injury and mortality in response to hyperoxia (Wang et al., 2004a), and their hearts were more vulnerable to ischemia-reperfusion injury (Nagy et al., 2006).

Recent studies from our laboratory also suggest an important role of Prdx6 in the skin. Initially, we identified Prdx6 as the product of a keratinocyte growth factor target gene in cultured keratinocytes (Frank et al., 1997). In vivo, overexpression of Prdx6 was found in the hyperproliferative epidermis of mouse skin wounds and of psoriatic patients as well as in cells of the wound granulation tissue (Frank et al., 1997; Munz et al., 1997). To determine the consequences of enhanced expression of Prdx6 in keratinocytes, we recently generated transgenic mice overexpressing this enzyme in the epidermis. Interestingly, the enhanced levels of Prdx6 protected keratinocytes from UVA and UVB toxicity in vitro and in vivo and accelerated wound closure in aged animals (Kumin et al., 2006). These results revealed that Prdx6 is rate-limiting in keratinocytes under stress conditions and suggested an important role of this enzyme in the skin. To address this question we performed UV irradiation and wound-healing studies with Prdx6 knockout mice (Wang et al., 2003), and we identified important functions of endogenous Prdx6 in UV protection and in blood vessel integrity in wounded skin.

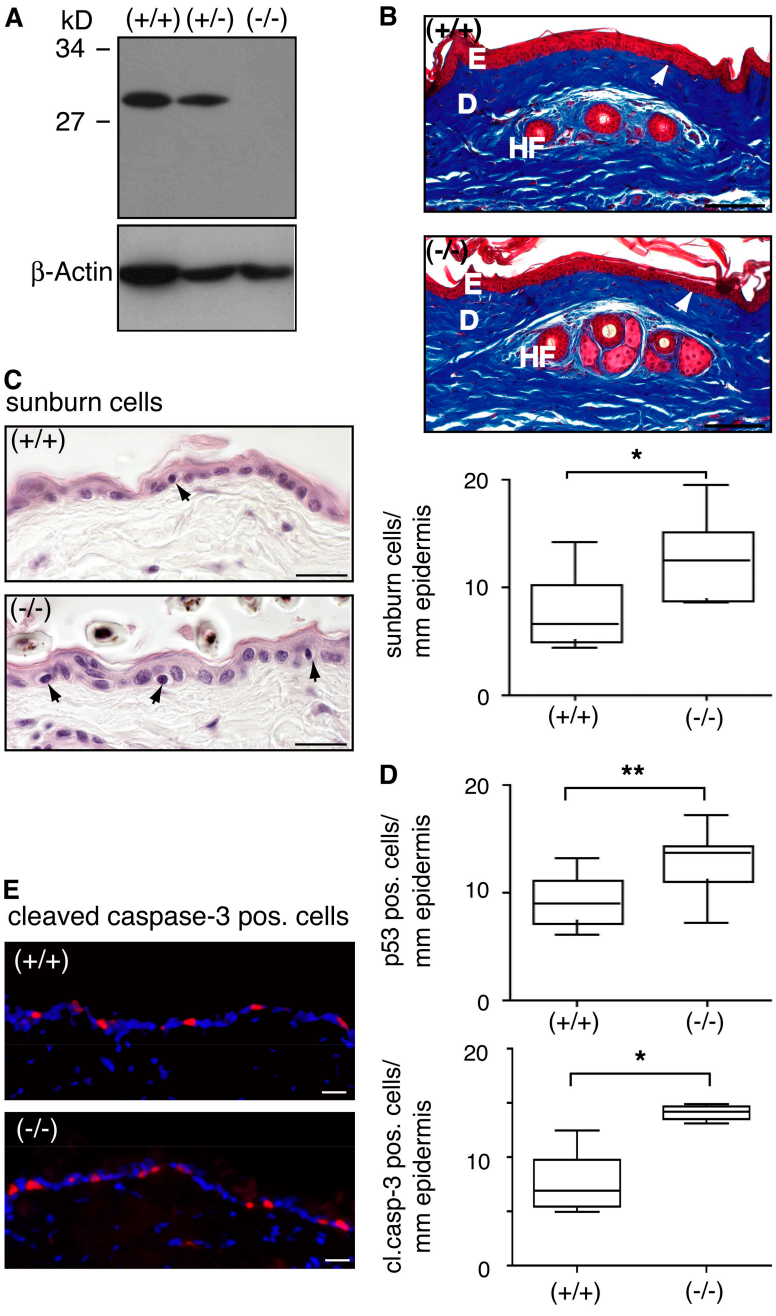

Figure 1. **Normal skin morphogenesis but enhanced UV susceptibility in Prdx6 knockout mice.** (A) Back skin lysates (30 μg protein) from homozygous (−/−) and heterozygous (+/−) Prdx6 knockout mice and wild-type controls (+/+) were analyzed by Western blotting for the presence of Prdx6 and β-actin. (B) Paraffin sections (6 μm) were stained using the Masson trichrome procedure. Bars indicate 100 μm. D: dermis; E: epidermis; HF: hair follicle. The basal cell layer of the epidermis is indicated with arrowheads. (C) Mice (n = 10 per genotype) were irradiated with 60 J/cm^2 UVA. Paraffin sections from the back skin of the irradiated mice were stained with H/E. Bars indicate 20 μm. Apoptotic sunburn cells in the epidermis (arrowheads) were counted. (D) Sections from UVA-irradiated mice (n = 10 per genotype) were stained with an antibody to p53, and p53-positive cells in the epidermis were counted. (E) Mice (n = 5 per genotype) were irradiated with 100 mJ/cm^2 UVB. Frozen sections from the back skin of the irradiated mice were analyzed by immunofluorescence using an antibody against cleaved caspase-3. Bars indicate 20 μm. Apoptotic cells in the epidermis were counted. Statistical analysis was performed using Mann-Whitney-U test for non-Gaussian distribution. *, P = 0.0146; **, P = 0.0068 (UVA irradiation) and *, P = 0.015 (UVB irradiation).

Results

Prdx6 is dispensable for skin morphogenesis and homeostasis

Before we challenged the knockout mice we confirmed the loss of Prdx6 in the skin by Western blot analysis of whole skin lysates (Fig. 1 A). No compensatory up-regulation of other cytosolic peroxiredoxins (Prdx1, Prdx2) and of the secretable Prdx4 was observed as determined by RNase protection assay (Table I). A detailed histological analysis of tail and back skin did not reveal any obvious abnormalities in the Prdx6 knockout mice (shown in Fig. 1 B for tail skin), demonstrating that Prdx6 is dispensable for skin morphogenesis and homeostasis.

Prdx6 protects from UVA- and UVB-mediated keratinocyte apoptosis

We next determined the role of endogenous Prdx6 in the response to physiological doses of UV. Upon irradiation with UVA, the number of apoptotic sunburn cells was significantly higher in the epidermis of UVA-irradiated Prdx6 knockout mice compared with wild-type controls ($n = 10$; Fig. 1 C). This result was confirmed by staining of UVA-irradiated skin sections with an antibody against p53, a protein, which is stabilized and activated upon DNA damage ($n = 10$; Fig. 1 D). Enhanced apoptosis in Prdx6-deficient epidermis was also observed after UVB irradiation as demonstrated by staining of UVB-irradiated skin for cleaved caspase-3 ($n = 5$; Fig. 1 E) and by analysis of sunburn cells in hematoxylin/eosin (H/E)-stained sections ($n = 5$; $P = 0.056$; unpublished data). These findings demonstrate that endogenous Prdx6 protects keratinocytes from UVA- and UVB-induced DNA damage and subsequent apoptosis.

Severe hemorrhage in wounds of Prdx6 knockout mice

We then subjected the Prdx6 knockout mice and their wild-type littermates to full-thickness excisional wounding. Although Prdx6 expression is particularly strong in keratinocytes of healing skin wounds (Munz et al., 1997), no obvious delay in wound reepithelialization was observed in the knockout mice (Fig. 2), and this was also confirmed by morphometric analysis (Fig. S1, available at http://www.jcb.org/cgi/content/full/jcb.200706090/DC1). We could not detect any histological abnormalities in the wound tissue up to d 3 after injury (Fig. 2 A). However, the granulation tissue of Prdx6 knockout mice was characterized by severe hemorrhage at d 5 after wounding (Fig. 2 B). This time point correlates with the phase of extensive wound angiogenesis. Hemorrhagic areas were present throughout the wound tissue, but were particularly large below the hyperproliferative epithelium (Fig. 2 B). They were seen in male and female knockout mice, but the phenotype was more pronounced in males (unpublished data). Hemorrhage was also occasionally observed in heterozygous animals (unpublished data). At d 8 after wounding, the hemorrhage was mostly resolved and only a few small affected areas remained (Fig. 2 C). Hemorrhage was no longer detectable at d 14 after wounding (Fig. 2 D). At this time point wounds in mice of both genotypes were fully healed. Despite the hemorrhage, no difference in the rate of wound closure, or in wound size and area of hyperproliferative epithelium was detected (Fig. S1). Furthermore, the rate of keratinocyte proliferation was unaltered (Fig. S1), and the inflammatory response was not obviously affected as determined by immunohistochemical staining for macrophages and neutrophils (unpublished data) and by expression analysis of the pro-inflammatory cytokine interleukin-1β (IL-1β) (Table I).

Endothelial cell damage and apoptosis in wounds of Prdx6 knockout mice

To unravel the reason for the severe hemorrhage, we stained the wound sections with an antibody against the endothelial cell-specific protein MECA-32 and determined the number and size of blood vessels in the wounds. However, we did not find a difference between knockout and wild-type animals (Fig. 3, A–C). Furthermore, maturation of blood vessels, which is reflected by the presence of surrounding smooth muscle cells, was also unaltered as determined by costaining for the endothelial cell marker PECAM-1 (CD31) and α-smooth muscle actin (α-SMA; Fig. 3 B). Consistent with these findings, expression of several genes encoding proteins involved in angiogenesis, e.g., vascular endothelial growth factor-A (VEGF-A), angiopoietins-1 and -2, and transforming growth factor β1 (TGF-β1) were normally expressed in unwounded and wounded skin of Prdx6 knockout mice (Table I). These findings suggest that the observed hemorrhage is not due to impaired angiogenesis or vessel maturation. Rather, defects in the endothelial cells themselves appeared likely.

Table I. **Expression of genes encoding proteins involved in angiogenesis, inflammation, or ROS detoxification is unaltered in normal and wounded skin of Prdx6-deficient mice.**

	skin		1dw		5dw		8dw		14dw	
Genotype	(+/+)	(−/−)	(+/+)	(−/−)	(+/+)	(−/−)	(+/+)	(−/−)	(+/+)	(−/−)
Prdx1	++++	++++	x	x	++++	++++	x	x	x	x
Prdx2	+++	+++	+++	+++	+++	+++	+++	+++	+++	+++
Prdx4	+	+	+	+	++	++	++	++	+	+
IL-1β	−	−	++++	++++	+++	+++	x	x	−	−
VEGF	+	+	x	x	++(+)	++(+)	x	x	x	x
Ang-1	+	+	x	x	(+)	(+)	x	x	x	x
Ang-2	(+)	(+)	x	x	+	+	x	x	x	x
TGF-β1	(+)	(+)	x	x	+(+)	+(+)	x	x	x	x

Expression levels were determined by RNase protection assays and are defined as: − not detectable, +: weakly expressed, ++: expressed at moderate levels, +++: strongly expressed, ++++: very strongly expressed. x, not tested. Ang = Angiopoietin.

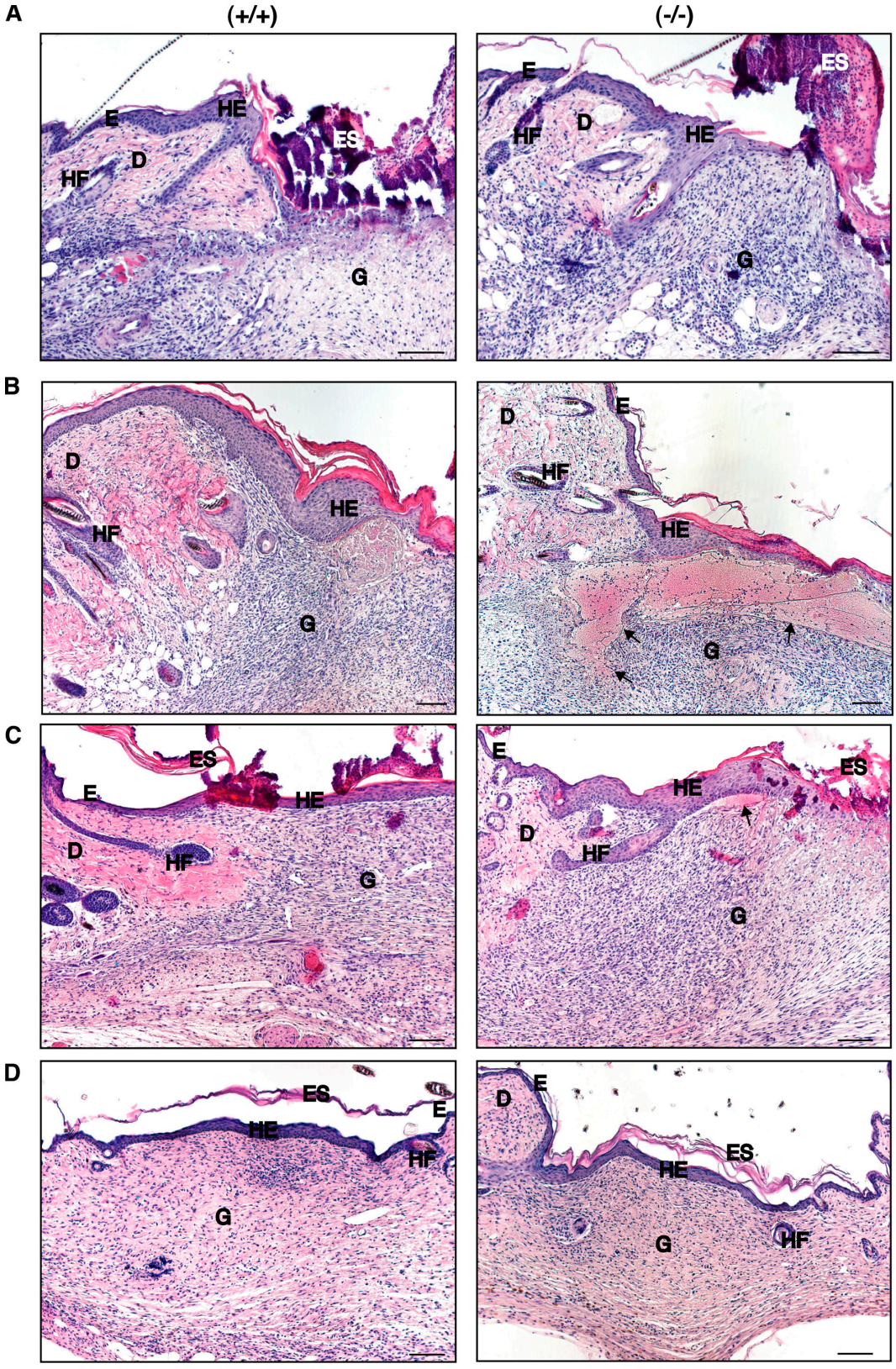

Figure 2. **Hemorrhage in 5-d wounds of Prdx6 knockout mice.** Full-thickness excisional wounds were generated on the back of Prdx6 knockout mice (−/−) and wild-type littermates (+/+). Sections from the middle of 3-d (A), 5-d (B), 8-d (C), and 14-d (D) wounds were stained with H/E. D: dermis, E: epidermis, Es: eschar, G: granulation tissue, HE: hyperproliferative wound epidermis, HF: hair follicle. Bars indicate 100 μm. Hemorrhage in the granulation tissue of knockout mice is indicated with arrows.

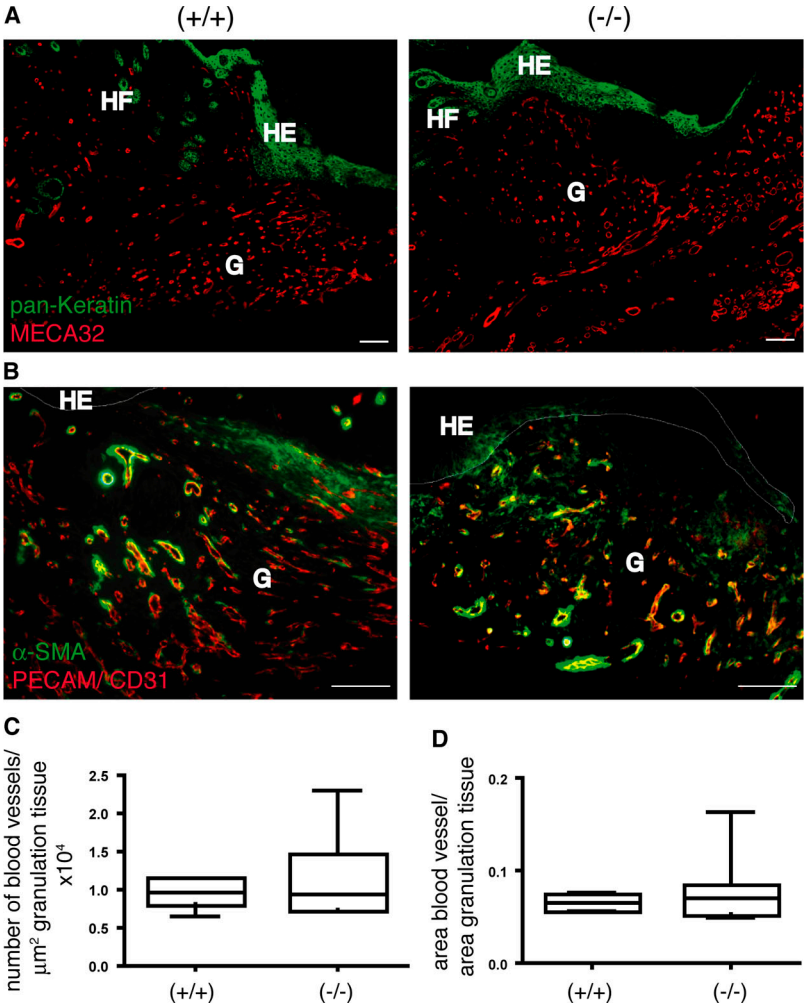

Figure 3. **Number, size and maturation of blood vessels are unaltered in 5-d wounds of Prdx6 knockout mice.** Paraffin sections from 5-d wounds of Prdx6 knockout mice and wild-type littermates were costained in A with antibodies against pan-keratin (green) and MECA-32 (red), and in B with antibodies against α-SMA (green) and PECAM-1/CD31 (red). Blood vessels that are surrounded by smooth muscle cells appear yellow. G: Granulation tissue, HE: hyperproliferative wound epidermis. Bars indicate 100 µm. C and D: Morphometric analysis of the newly formed blood vessels in 5 d wounds of wild-type and Prdx6 knockout mice using the Openlab software. The number of blood vessels/µm^2 granulation tissue (C) and the area covered by blood vessels (µm^2) in relation to the total area of granulation tissue (µm^2) (D) was analyzed in 7 wounds from wild-type mice and 9 wounds from Prdx6 knockout mice.

This hypothesis was confirmed by analysis of semi-thin sections from the wound tissue and in particular by electron microscopy. In the wounds of control mice, open and well-structured blood vessels had formed (Fig. 4, A and C), whereas wounds of Prdx6 knockout mice showed strongly damaged blood vessels (Fig. 4, B, D, E, and F), and vacuoles were present in the cytoplasm of endothelial cells. Furthermore, damaged blood vessels were surrounded by extravasated erythrocytes, reflecting the hemorrhage (Fig. 4 D), and erythrocytes were also present in the wound epidermis of the knockout mice (Fig. 4 H), but not of wild-type controls (Fig. 4 G). A semi-quantitative analysis of the semi-thin sections revealed that more than 50% of the vessels were defective in the superficial granulation tissue, adjacent to the wound epidermis. In the middle of the granulation tissue 10–50% of the vessels were affected, whereas less than 10% of the vessels were damaged in the lowest part of the wound (Fig. 5 A).

The ultrastructural appearance of the endothelial cells suggested that some of them are apoptotic. This was confirmed by double-immunofluorescence staining with antibodies against PECAM-1 and cleaved caspase-3. At d 5 after wounding, apoptotic endothelial cells were detected in some blood vessels in the granulation tissue below the hyperproliferative epidermis, and their number was significantly increased in the knockout mice compared with wild-type controls (Fig. 5, B and C). This result is consistent with the histological appearance of the endothelial cells in semi-thin sections, although the percentage of morphologically damaged endothelial cells was much higher compared with the percentage of cleaved caspase-3–positive cells. This suggests that at least some of the damage may be reversible and does not lead to cell death.

In addition to the endothelial cells, some fibroblasts and granulocytes in the granulation tissue of Prdx6 knockout mice also appeared damaged (Fig. 4 B and unpublished data). However, ~90% of all cleaved caspase-3 positive cells in the wound were also PECAM-1 positive, demonstrating that endothelial cells are particularly affected (unpublished data).

The endothelial cell damage was still detectable at d 8 after wounding, but to a much lesser extent (Fig. S2, B and D; available at http://www.jcb.org/cgi/content/full/jcb.200706090/DC1). This is also reflected by the reduced hemorrhage at this later stage of healing (Fig. 2 C). Endothelial cells from vessels, which were already surrounded by perivascular cells (Fig. S2 D), appeared less damaged compared with those of immature vessels (Fig. S2 B).

Enhanced oxidative stress in wounds of Prdx6 knockout mice

We next determined if the extent of hemorrhage correlates with the severity of oxidative stress at the wound site. For this purpose

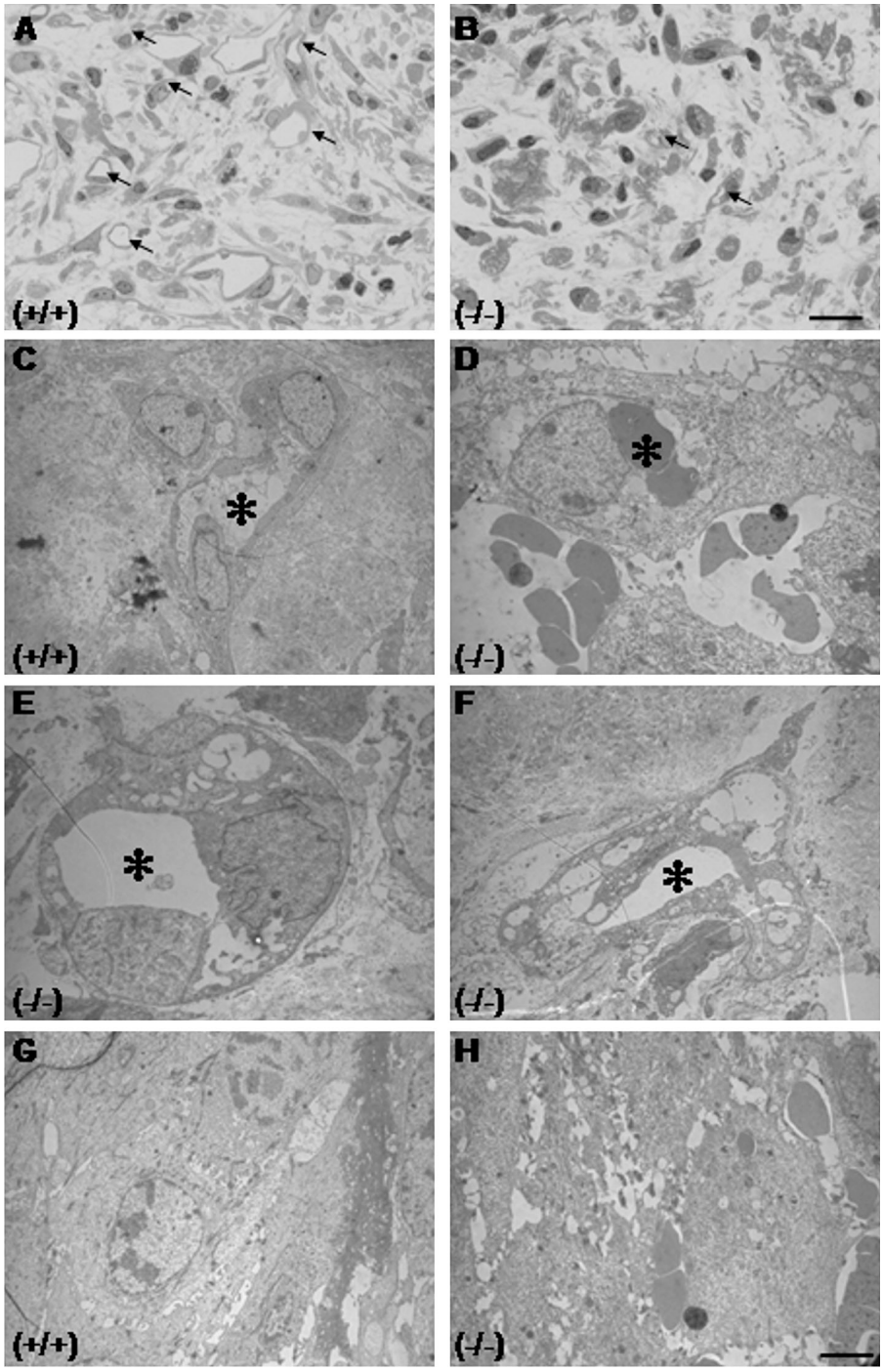

Figure 4. **Endothelial cell damage in 5-d wounds of Prdx6 knockout mice.** Methylene-blue stained, semi-thin sections (A and B) and electron micrographs of newly formed blood vessels (C–F) from 5-d wounds of control (A and C) and Prdx6 knockout mice (B, D, E, and F) are shown. Open and well-structured blood vessels are present in control mice (A), while wounds of Prdx6 knockout mice show strongly damaged vessels (B, arrows) with vacuolized endothelial cells (E and F). A well-structured capillary is visible in a control wound (C), while an erythrocyte-filled capillary with strong signs of endothelial cell damage is present in the wound of a Prdx6 knockout mouse. The damaged vessel is surrounded by extravasated erythrocytes (D). Electron micrographs of newly formed epidermis in wounds of control (G) and Prdx6 knockout (H) mice are shown. Erythrocytes are present between the keratinocytes of the newly formed epidermis in wounds of Prdx6 knockout mice. Bars: A and B = 25 μm; C–H = 5 μm.

we performed oxyblot analyses with lysates from pooled wounds of different animals to determine the levels of oxidized proteins, which are characterized by the presence of carbonyl groups. In three independent experiments with different wound lysates, 5-d wounds of knockout mice had a consistently higher protein carbonyl content compared with wild-type controls (Fig. 6 A). Protein oxidation was more pronounced in male animals, consistent with the more severe phenotype seen in Prdx6 knockout mice. In addition, staining with an antibody against nitrotyrosine, which reflects formation of the toxic peroxinitrite from nitric oxide and superoxide anions, revealed a significantly increased number of nitrotyrosine positive cells in wounds of Prdx6 knockout mice (Fig. 6, B and C). Collectively, oxidative stress is obviously enhanced in wounds of Prdx6-deficient animals, and the elevated levels of ROS are likely to damage endothelial cells.

Knock-down of Prdx6 in endothelial cells enhances their susceptibility to ROS toxicity

To determine if the lack of Prdx6 in endothelial cells is indeed deleterious under conditions of oxidative stress, we studied the consequences of siRNA-mediated Prdx6 knock-down on the

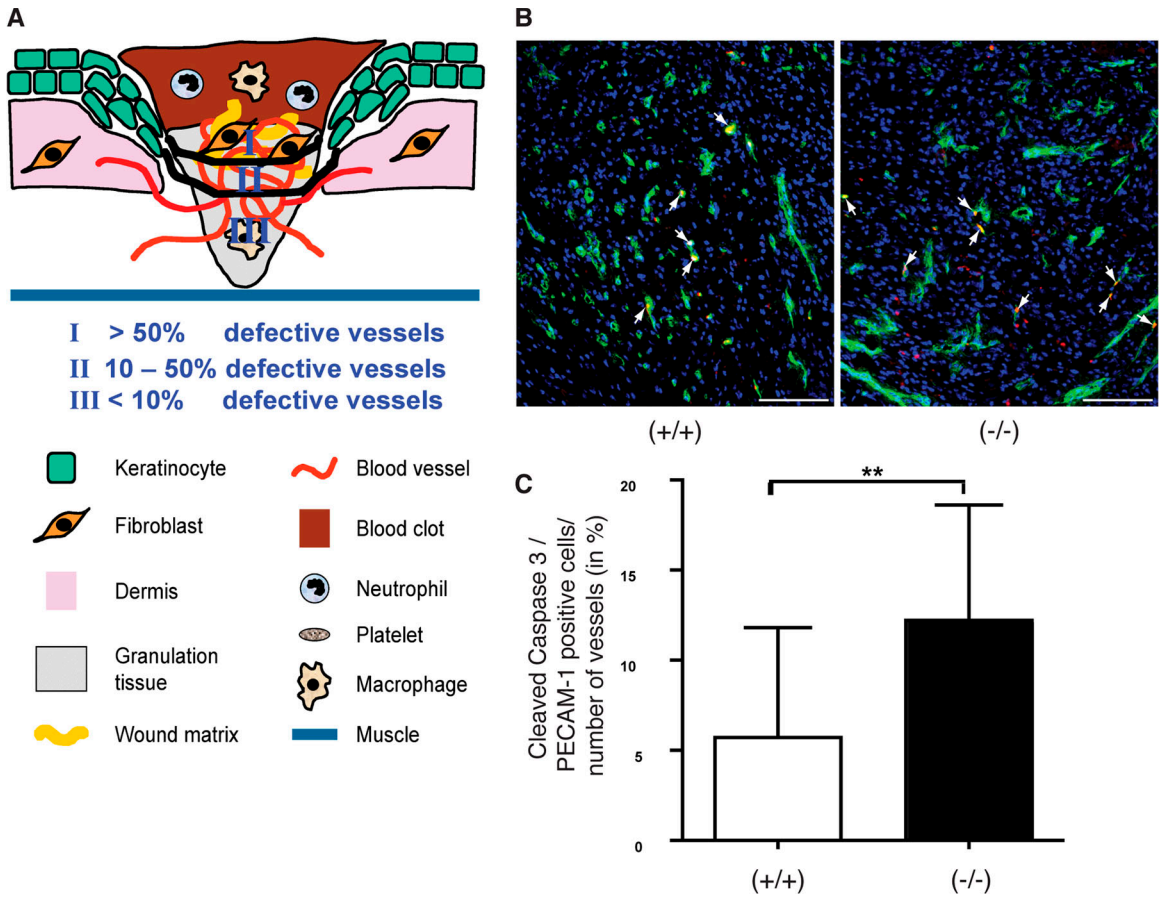

Figure 5. **Enhanced apoptosis of endothelial cells and localization of defective blood vessels in 5-d wounds of Prdx6 knockout mice.** (A) In zone I, directly below the hyperproliferative epithelium, more than 50% of the blood vessels were damaged in Prdx6 knockout mice as determined by analysis of semi-thin sections (see Fig. 4). In zone II, 10–50% defective vessels were found, whereas in zone III less than 10% of the blood vessels were damaged. (B and C) Cryosections from the middle of 5-d wounds were costained with antibodies against cleaved caspase-3 (red) and PECAM-1 (green) (B). Arrows indicate apoptotic endothelial cells (yellow). Bars indicate 100 µm. The total number of PECAM-1 positive blood vessels as well as the number of cleaved caspase-3/PECAM-1 double-positive cells were determined in the granulation tissue below the hyperproliferative epithelium. Cells and vessels in one microscopic field (200×) per wound halve were counted. The percentage of blood vessels that contained apoptotic endothelial cells is indicated on the y-axis. 21 wound halves from 13 wild-type animals and 20 wound halves from 11 knockout mice were analyzed. Statistical analysis was performed with GraphPad Prism4 software, using the Mann-Whitney-U test for non-Gaussian distribution. **, $P = 0.0031$.

survival of cultured human umbilical vein endothelial cells (HUVEC) in response to ROS treatment. Efficient knock-down was achieved with three different Prdx6 siRNAs, whereas random siRNAs had no effect (Fig. 7 A). The knock-down of Prdx6 did not affect cell viability under normal culture conditions, but Prdx6 siRNA treatment strongly reduced the viability of HUVEC cells upon treatment with either hydrogen peroxide or glucose oxidase in comparison to random siRNA-treated cells (Fig. 7 B). These results were reproduced in 9 independent experiments with two different siRNA sequences against Prdx6 (#79, #81) and in four independent experiments with siRNA #80. Based on these in vitro results and the hemorrhage observed in wounds of Prdx6 knockout mice we conclude that endogenous Prdx6 is required for survival of endothelial cells under conditions of oxidative stress.

Bone marrow chimeras reveal that Prdx6 deficiency in hematopoietic and resident cells contributes to wound hemorrhage

Finally, we determined if the loss of Prdx6 in endothelial cells is solely responsible for the phenotype or if enhanced levels of ROS produced by Prdx6-deficient inflammatory cells also contribute to the endothelial cell damage. The latter possibility was suggested by the finding that macrophages from Prdx6 mice have higher levels of intracellular ROS (Wang et al., 2003), and at least hydrogen peroxide can be released into the surrounding extracellular space and possibly damage endothelial cells. To address this question we generated bone-marrow chimeric mice. Wild-type and Prdx6-deficient female mice were subjected to 950 rad gamma-irradiation to destroy the hematopoietic cells in the bone marrow. The irradiated mice subsequently received bone marrow cells from either wild-type or knockout donors. Male mice were used as bone marrow donors to allow subsequent identification of hematopoietic cells through the presence of the Y chromosome. 6 wk after irradiation and bone marrow transfer the fur of the treated mice had turned gray (Fig. S3 A, available at http://www.jcb.org/cgi/content/full/jcb.200706090/DC1). At this time point successful reconstitution of the hematopoietic system was verified by semi-quantitative PCR of blood cell DNA using primers specific for the Y-chromosome DNA (Fig. S3 B). 10 wk after irradiation this result was confirmed for

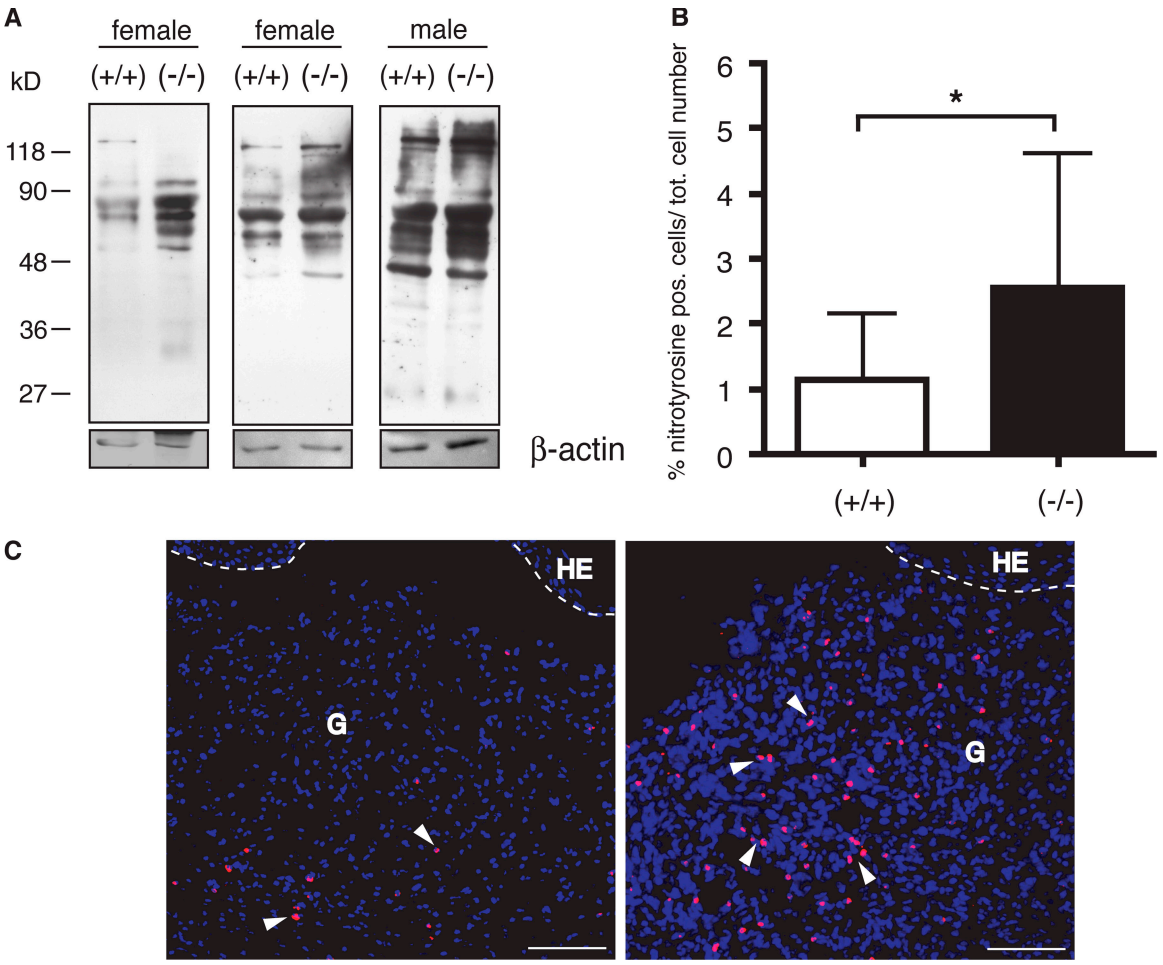

Figure 6. **Enhanced oxidative stress in 5-d wounds of Prdx6 knockout mice.** (A) Lysates of 5-d wounds from female and male mice (female 18.3 μg and 10 μg, male 20 μg of total protein) were analyzed for the presence of oxidized proteins by oxyblot analysis. The membrane was reprobed with an antibody to β-actin. (B) 12 wound halves of 9 female wild-type mice and 12 wound halves of 9 female knockout mice were analyzed by immunofluorescence for the presence of nitrotyrosine positive cells. The percentage of nitrotyrosine positive cells was determined using the ImageJ program. Statistical analysis was performed using the Mann-Whitney-U test. *, $P = 0.0464$. Representative stainings are shown in C. Nitrotyrosine-positive cells are indicated by arrowheads. Nuclei were counterstained with Hoechst. Bars indicate 50 μm. G: Granulation tissue, HE: Hyperproliferative epithelium.

DNA from bone marrow (Fig. S3 C). To estimate the efficiency of bone marrow transplantation, we performed real-time PCR with DNA from blood cells at wk 6 after bone marrow transplantation. In all female recipients the amount of Y chromosome DNA reached 70% or more of the amount present in DNA from male mice (Fig. S3 D).

Chimeras were subjected at wk 10 after bone marrow transplantation to full-thickness excisional wounding. This late time point was chosen to ensure full reconstitution of the hematopoietic system at the time of wounding. Nevertheless, the bone marrow transplantation procedure delayed the wound healing process in mice with all genotype combinations, possibly due to irradiation-induced tissue damage and/or enhanced stress of the mice. Therefore, only a small area of the clot was replaced by highly cellular granulation tissue, and angiogenesis was hardly detectable in 5-d wounds. This time point was therefore too early to detect damaged blood vessels (unpublished data). We subsequently repeated the experiment and analyzed the wounds at d 7 after injury. Western blot analysis of wound lysates confirmed that wild-type hematopoietic cells had infiltrated the wound tissue of Prdx6-deficient recipient mice. Thus, Prdx6 protein was detected in lysates of 7-d wounds from transplanted Prdx6 knockout mice, which had received bone marrow from wild-type mice, whereas Prdx6 protein was not detectable in normal back skin lysates of these mice (Fig. 8 A). The severe hemorrhage in the granulation tissue and the presence of extravasated erythrocytes in the wound epidermis were confirmed in wounds of Prdx6 knockout mice, which had received Prdx6-deficient bone marrow (Fig. 8, B and C; ko/ko; $n = 7$). In these mice, the number of apoptotic endothelial cells was significantly enhanced compared with wild-type mice, which had received wild-type bone marrow (data not shown). Mild hemorrhage was observed in most Prdx6 knockout mice that had received wild-type bone marrow (Fig. 8, B and C; ko/wt; $n = 8$) and in most wild-type mice with Prdx6-deficient bone marrow (Fig. 8, B and C; wt/ko; $n = 5$). In both treatment groups, the number of apoptotic endothelial cells was also increased, although the difference was not statistically significant (unpublished data). As expected, hemorrhage was absent or very mild in wild-type mice with wild-type bone marrow (Fig. 8, B and C; wt/wt; $n = 6$). The intensity

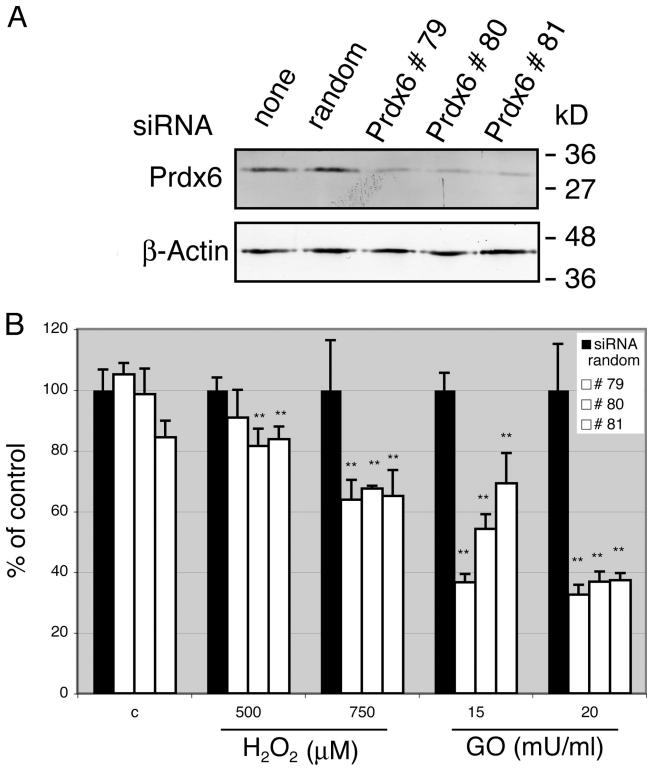

Figure 7. **Enhanced ROS susceptibility of HUVEC after siRNA-mediated knock-down of Prdx6.** HUVEC were transfected with different siRNAs against Prdx6 or random siRNA. Efficient Prdx6 knockdown was verified by Western blot analysis (A). Cells transfected in parallel plates were subsequently challenged with different concentrations of hydrogen peroxide or glucose oxidase (GO) or solvent control, and subjected to MTT assay (B). All measurements were performed in quadruplicates ($n = 4$). The values obtained with random siRNA-transfected cells were arbitrarily set as 100. Statistical analysis was performed using the GraphPad Prism4 software and applying the One-way ANOVA analysis followed by the Dunnett's Multiple Comparison Test. One-way analysis: **, $P = 0.0046$ for 500 μM H_2O_2, ***, $P = 0.0005$ for 750 μM H_2O_2 and ***, $P < 0.0001$ for 15 and 20 mU/ml GO. Dunnett's Multiple Comparison: **, $P < 0.01$ for all treatment groups, except for siRNA random versus #79 at a concentration of 500 μM H_2O_2 ($p > 0.05$).

of the hemorrhage phenotype in the different treatment groups was confirmed by immunostaining for fibrin. In all mice, fibrin staining was seen in the middle of the wound, where the original clot was not yet replaced by mature granulation tissue (unpublished data). However, in most of the mice, which had Prdx6-deficient inflammatory cells or resident cells or both, intermediate or strong fibrin staining was also seen in the mature granulation tissue underneath the hyperproliferative epithelium (Fig. 8 D). This reflects the necessity to rapidly seal damaged vessels with a blood clot in order to avoid excessive bleeding. By contrast, fibrin deposition was absent or much less pronounced in wild-type mice with wild-type bone marrow (Fig. 8 D). At the ultrastructural level (Fig. S4, available at http://www.jcb.org/cgi/content/full/jcb.200706090/DC1), damage of endothelial cells as well as morphological abnormalities in some fibroblasts and granulocytes were detected in all animals with Prdx6-deficient cells (Fig. S4, C–F). Again, the most striking phenotype was observed when both hematopoietic and resident cells lacked Prdx6. Collectively, this in vivo experiment revealed that the presence of Prdx6 is required in inflammatory cells as well as in resident cells for blood vessel integrity in wounded skin (shown schematically in Fig. 9).

Discussion

The skin is frequently challenged by UV irradiation or by toxic chemicals. These insults induce the formation of ROS, which damage cellular macromolecules, leading to premature aging or even carcinogenesis (Cerutti and Trump, 1991). Large amounts of ROS are also generated by inflammatory cells in injured tissues as a defense against invading bacteria. Therefore, cells had to develop strategies to detoxify ROS. In recent years, peroxiredoxins have emerged as key players in the ROS defense, in particular under stress conditions (Hofmann et al., 2002). It is therefore of particular interest to determine their roles in normal, wounded, and diseased skin.

Prdx6 protects keratinocytes from UV-induced cell damage

The results presented in this study reveal an important role of Prdx6 in skin protection from UV toxicity. Because UV, in particular UVA, exerts its damaging effect at least in part through induction of ROS formation (Sander et al., 2004), it seems likely that Prdx6 directly detoxifies the newly formed ROS as well as the resulting lipid peroxides. Therefore, UV-mediated damage of cellular macromolecules, including DNA damage, is probably enhanced in the absence of Prdx6. This hypothesis is supported by the increase in p53-positive keratinocytes in UVA-irradiated skin of Prdx6 knockout mice compared with control animals. These results suggest that activation of Prdx6 expression and/or activity may be a promising strategy for skin protection under stress conditions.

Prdx6 is dispensable for wound reepithelialization but required for blood vessel integrity in wounded skin

Prdx6 is highly expressed in keratinocytes of healing skin wounds (Munz et al., 1997). Interestingly, Prdx6 levels are rate limiting in the wound epidermis of aged animals because keratinocyte-specific overexpression of Prdx6 enhanced wound closure in old mice (Kumin et al., 2006). Therefore, it was surprising that reepithelialization occurred normally in Prdx6 knockout mice. The most likely explanation is the abundance of other ROS-detoxifying enzymes and antioxidant proteins in wound keratinocytes (Steiling et al., 1999; Hanselmann et al., 2001), which may compensate for the lack of Prdx6. This compensation is obviously not sufficient in other cells as reflected by the severe hemorrhage in wounds of Prdx6-deficient mice. Because Prdx1 and Prdx2 knockout mice show erythrocyte defects (Lee et al., 2003; Neumann et al., 2003), and because exogenous Prdx6 prevented methemoglobin formation in erythrocyte hemolysates (Stuhlmeier et al., 2003), hematopoietic abnormalities may be responsible for the hemorrhage phenotype. However, a total blood analysis of five age-matched female animals per genotype did not reveal obvious differences in the shape or number of erythrocytes, and hematocrit as well as hemoglobin

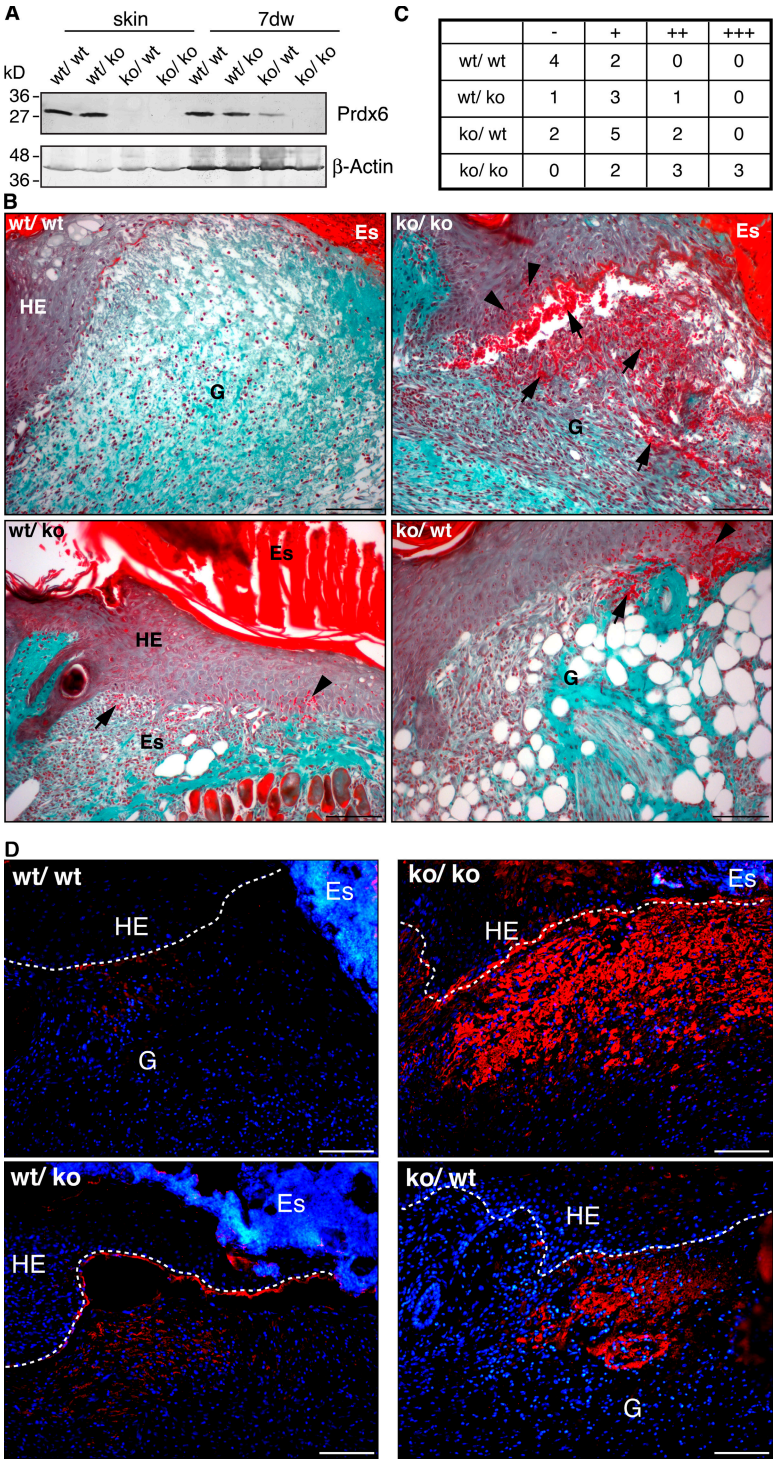

	-	+	++	+++
wt/ wt	4	2	0	0
wt/ ko	1	3	1	0
ko/ wt	2	5	2	0
ko/ ko	0	2	3	3

Figure 8. **Prdx6-deficiency in hematopoietic cells and in resident cells contributes to endothelial cell damage in wounded skin.** (A) Lysates from nonwounded skin and from 7-d wounds (50 μg protein) of different bone marrow chimeric mice were analyzed by Western blotting for the presence of Prdx6 and β-actin. (B) Paraffin sections (6 μm) from the middle of 7-d wounds were stained using the Masson Goldner procedure. Wt/wt; wild-type mice with wild-type bone marrow; wt/ko; wild-type mice with knockout bone marrow; ko/wt: knockout mice with wild-type bone marrow; ko/ko: knockout mice with knockout bone marrow. Arrows indicate hemorrhage; arrowheads indicate extravasated erythrocytes in the hyperproliferative epithelium. (C) Semi-quantitative analysis of the intensity of the hemorrhage seen in Masson Goldner stained sections (judged by two independent investigators): hemorrhage not detectable, +: weak, ++: intermediate, +++: strong. Numbers indicate the number of animals analyzed; 1–2 wounds per animal. (D) Paraffin sections (6 μm) from the middle of 7-d wounds of bone marrow chimeric mice were stained with an antibody against fibrinogen/fibrin (red). Nuclei were counterstained with Hoechst (blue). Bars in B and D indicate 100 μm. Es: Eschar, G: Granulation tissue, HE: Hyperproliferative wound epidermis.

concentration were also unaltered (unpublished data). Furthermore, blood clotting was not impaired because no bleeding abnormalities were seen immediately after injury (unpublished data). Consistent with the latter finding, the number of thrombocytes was similar in Prdx6-deficient mice and wild-type controls (unpublished data). Finally, the bone marrow transplantation experiments confirm that hematopoietic cells are not solely responsible for the hemorrhage, because transplantation of Prdx6-deficient bone marrow cells into wild-type animals generated only a mild phenotype. By contrast, the onset of hemorrhage correlated with the formation of new blood vessels, suggesting that Prdx6 is required for endothelial cell integrity and viability in the wound tissue. Indeed, this hypothesis was proven by ultrastructural analysis of the newly formed blood vessels. The endothelial cell damage is likely to cause transient leakiness of blood vessels, resulting in local hemorrhage. Because we did not observe continuous bleeding and subsequent death of the animals, the defective vessels appear to be rapidly sealed by blood clotting as reflected by the enhanced fibrin staining in the granulation tissue of knockout mice (Fig. 8 D).

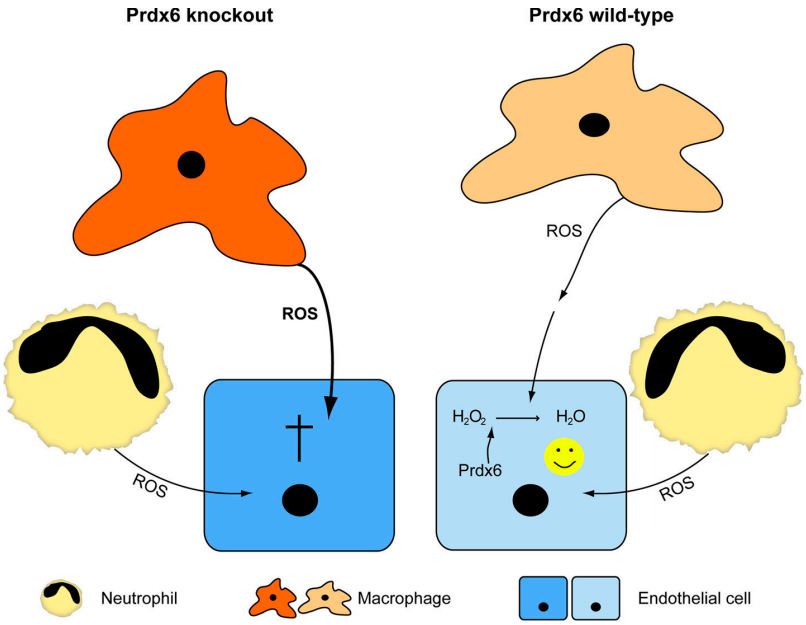

Figure 9. **Schematic representation of the role of Prdx6 in the ROS-mediated interplay between inflammatory cells and endothelial cells.** Right hand side: in wild-type mice, ROS are produced by macrophages and neutrophils, released from these cells, and taken up by endothelial cells. In the cytoplasm of the latter, hydrogen peroxide and organic peroxides are detoxified by Prdx6, resulting in cell survival. Left hand side: Prdx6-deficient inflammatory cells have enhanced levels of ROS, which damage adjacent endothelial cells. Because the latter also lack Prdx6, detoxification of hydrogen peroxide and organic peroxides is impaired, resulting in cell damage and apoptosis.

Enhanced oxidative stress in wounds of Prdx6 knockout mice is responsible for the endothelial cell damage

In contrast to the vessels in the wound, those in normal skin were not affected. Furthermore, the hemorrhage phenotype was not observed in Prdx6-deficient embryos at E13.5, where massive angiogenesis in different organs occurs (Fig.S5, available at http://www.jcb.org/cgi/content/full/jcb.200706090/DC1; and unpublished data). This finding suggests that the loss of Prdx6 only affects endothelial cells under conditions, which are associated with oxidative stress, such as inflammation. Under these circumstances, invading phagocytic cells produce high levels of superoxide anions through the action of NADPH oxidases (Bedard and Krause, 2007). Superoxide anions, in turn, are rapidly dismutated to hydrogen peroxide. The latter may then penetrate the endothelial cell membrane and damage endothelial cells (Fig. 9). In addition, a very recent study demonstrated that even superoxide anions can cross the endothelial membrane through chloride channels (Hawkins et al., 2007), thereby further enhancing the oxidative stress in these cells. The capability of endothelial cells to take up superoxide anions may at least in part explain the enhanced vulnerability of Prdx6-deficient endothelial cells compared with other cell types in the wound tissue. Alternatively, endothelial cells may express lower levels of other ROS-detoxifying enzymes, and we currently investigate this possibility. The important role of Prdx6 for endothelial cell survival under conditions of oxidative stress is also reflected by the correlation between inflammation and endothelial cell damage. Thus, more severe hemorrhage was seen in wounds of male mice that are characterized by a stronger inflammatory response (Ashcroft and Mills, 2002) and higher levels of ROS (Fig. 6). In addition, endothelial cells in the superficial granulation tissue, where ROS-producing neutrophils are still abundant at d 5 after injury, were particularly affected. Finally, the vessel defects were reversible and disappeared with the decrease in wound inflammation. The stabilization of the newly formed vessels by perivascular cells may further contribute to the reversibility because the defects were milder in vessels that were already surrounded by pericytes and smooth muscle cells (Fig. S2) and thus more protected from inflammatory cell-derived ROS. A role of Prdx6 in endothelial cell protection under stress conditions is further supported by our in vitro experiments, which demonstrated that knock-down of Prdx6 does not affect the viability of these cells under normal culture conditions, but in response to oxidative stress.

ROS-mediated cross-talk between hematopoietic cells and endothelial cells in healing skin wounds

Damage of Prdx6-deficient endothelial cells is likely to be further accelerated in the knockout mice through enhanced ROS production by inflammatory cells. Thus, macrophages from Prdx6-deficient mice have higher levels of intracellular ROS (Wang et al., 2003). This is reflected by the enhanced production of the ROS-inducible enzyme matrix metalloproteinase 9 by Prdx6-deficient macrophages, which was reversible by treatment with antioxidants (our own unpublished data). Some of the macrophage-derived ROS, in particular the noncharged hydrogen peroxide, are likely to be released into the immediate environment, resulting in damage of neighboring cells. In addition, Prdx6-deficiency may increase NADPH oxidase activity in macrophages. Thus, lipopolysaccharide-mediated activation of NADPH oxidase was enhanced in macrophages of Prdx2 knockout mice, and this effect was mediated by elevated levels of intracellular hydrogen peroxide (Yang et al., 2007). Although we did not observe a higher number of macrophages in wounds of Prdx6-deficient mice (data not shown), the elevated levels of ROS released by the available macrophages may further enhance the oxidative stress at the wound site (Fig. 9). Consistent with this assumption, the levels of oxidized proteins were enhanced in the wound tissue of Prdx6 knockout mice, and more nitrotyrosine positive cells were also detected, reflecting enhanced levels

of peroxinitrite. This toxic molecule has also been identified as a substrate of Prdx6, suggesting that it accumulates in Prdx6-deficient mice and further contributes to endothelial cell damage (Peshenko and Shichi, 2001). Most importantly, the hypothesis that hematopoietic cells contribute to the hemorrhage phenotype is strongly supported by the analysis of wounds that had been generated in bone marrow chimeras. The invading ROS-producing macrophages and neutrophils are likely to be responsible for this damaging effect, but a contribution of bone marrow-derived endothelial progenitor cells cannot fully be excluded. These cells can be incorporated into newly formed blood vessels at the wound site (Asahara et al., 1999; Crosby et al., 2000), in particular under ischemic conditions (Tepper et al., 2005). However, in nonischemic wounds of wild-type mice, the contribution of these cells to the formation of wound vessels is minor (Montesinos et al., 2004; Tepper et al., 2005; Bluff et al., 2007). Therefore, it seems likely that the damaging effect of Prdx6-deficient bone marrow cells on the wound vasculature is predominantly due to the secretion of ROS by inflammatory cells. This suggests that Prdx6 may also be required for blood vessel integrity in other situations of inflammation-associated angiogenesis, in particular in cancer.

Collectively, these studies revealed that endogenous Prdx6 protects the epidermis from UV-induced damage. In addition, they demonstrate the requirement of this enzyme in hematopoietic cells and resident cells for the integrity of newly formed blood vessels in inflamed tissues. Finally, they provide insight into the cross-talk between hematopoietic and resident cells at the wound site and the role of ROS in this interplay.

Materials and methods

siRNA transfection of HUVEC

HUVEC (Clonetics) were seeded on collagen A (10 μg/ml, Biochrom AG) coated dishes and cultured in endothelial growth medium EGM-2 (Clonetics). Synthetic siRNAs dissolved in RNase-free PBS were combined 1:1 to a final concentration of 50 μM, incubated at 50°C for 2 min in annealing buffer (25 mM NaCl, 5 mM $MgCl_2$), and cooled down to room temperature. 3500 HUVEC/well were seeded into 96-well plates. 24 h later they were transfected with Prdx6 or random siRNAs (30 nM each) for 48h. Protein lysates were analyzed by Western blotting for the levels of Prdx6 and β-actin.

For siRNA lipid complex formation, 10 μl growth medium without any additives but with 10 mM Hepes and siRNA (30 nM) were placed into polystyrene tubes and vigorously mixed. After the addition of 10 μl complex medium and the lipid Atufect 01 (1.2 μg/ml; Atugen AG), the components were incubated at 37°C in 95% relative air humidity and 5% CO_2 for 30 min. Thereafter, this mixture was added to the cells, which had previously received 80 μl fresh growth medium.

Sequences of Prdx6 siRNAs: # 72279 A, 5′-GACTTTACCCCAGTGTGCA-3′; # 72279 B, 5′-TGCACACTGGGGTAAAGTC-3′; # 72280 A, 5′-CTGAAGCTGTCTATCCTCT-3′; # 72280 B, 5′-AGAGGATAGACAGCTTCAG-3′; # 72281 A, 5′-CTTTCAATAGACAGTGTTGA-3′; # 72281 B, 5′-TCAACACTGTCTATTGAAAG-3′; siRNA random (QIAGEN) sense, 5`-UUCUCCGAACGUGUCACGUdTdT-3; antisense, 5`-ACGUGACACGUUCGGAGAAdTdT-3

Survival assay

Cells were grown for 2 d in growth medium including the siRNA, and treated for 7 h with 500 or 750 μM hydrogen peroxide or with 15 or 20 mU/ml glucose oxidase. Cell viability was quantified using the 3-(4,5-dimethylthiazol-2-yl)-2,5-diphenyl-tetrazolium bromide (MTT) assay (Kumin et al., 2006).

Animals

Mice were housed and fed according to federal guidelines, and all procedures were approved by the local veterinary authorities (Zurich, Switzerland).

Wounding and preparation of wound tissues

Mice were anaesthetized by intraperitoneal injection of ketamine/xylazine. Two 5-mm full-thickness excisional wounds were made on either side of the dorsal midline (Werner et al., 1994). Complete wounds including 2 mm of the epithelial margins were excised and frozen in liquid nitrogen. Alternatively, wounds were fixed overnight in 95% ethanol/1% acetic acid or in 4% paraformaldehyde (PFA)/PBS, followed by paraffin embedding, or directly embedded in tissue-freezing medium. Sections (6 μm) from the middle of the wound were stained with hematoxylin/eosin (H/E), by the Masson trichrome procedure or with the Masson-Goldner staining kit (Merck), or used for immunofluorescence/immunohistochemistry. Only littermates or at least age-matched animals of the same sex were used for direct histological comparison.

UV irradiation of mice

Mice were anaesthetized, shaved, and irradiated with 60 J/cm^2 UVA or with 100 mJ/cm^2 UVB as described by Kumin et al. (2006). 24 h later they were killed and the tissue was fixed in 4% PFA. To identify apoptotic "sunburn" cells PFA-fixed paraffin sections were stained with H/E. Alternatively, frozen sections were analyzed by immunofluorescence with an antibody against cleaved caspase-3 (see below). The number of apoptotic keratinocytes per mm of basement membrane was determined by two (UVB) or three (UVA) independent investigators. For this purpose cells were counted in 10–15 independent microscopic fields per mouse or along the entire epidermis present on the section.

Generation of bone marrow chimeras

Female mice (9–11-wk old) were irradiated (950 rad-γ) and subsequently 5–7 × 10^6 bone marrow cells that were flushed from tibiae and femurs of wild-type and knockout male donor mice were intravenously injected. Wild-type and knockout mice received bone marrow from either wild-type or knockout male mice. After transplantation mice were maintained in a laminar flow environment. They received sterilized food and water, which was supplemented with antibiotics (Borgal, 0.1%) for 2 wk. 6 wk after transplantation genomic DNA from blood cells was tested by semi-quantitative PCR for the presence of the Y chromosome (Kunieda et al., 1992) and by Real-time PCR using SYBR green (Applied Biosystems) and primers described elsewhere (Wang et al., 2002). Assays were performed twice in duplicate and evaluated by the Δct-method as described by the manufacturer (Applied Biosystems). 10 wk after transplantation the wound healing experiment was performed. After sacrifice, bone marrow was taken, and the presence of the Y chromosome in DNA of bone marrow cells was verified by semi-quantitative DNA.

Electron microscopy

Mice were lethally anesthetized with pentobarbital (700 mg/kg) and perfused with 4% PFA in PBS. Wounds were kept overnight in fixation solution, rinsed, and stored in PBS. Before embedding, the wound samples were treated with 2% OsO_4 for 2 h. After washing, they were stained in 1% uranyl acetate, dehydrated through series of graded ethanols and embedded in araldite resin. Semi-thin sections (500 nm) were cut with a glass knife and stained with methylene blue. Ultra-thin sections (30–60 nm) were processed with a diamond knife and placed on copper grids. Transmission electron microscopy was performed using a 902A electron microscope (Carl Zeiss, Inc.).

RNA isolation and RNase protection assay

RNA isolation and RNase protection assay were performed as described (Chomczynski and Sacchi, 1987; Werner et al., 1993). All protection assays were performed at least in duplicate with different sets of RNAs from independent experiments. A murine *prdx2* cDNA fragment (nt 310–555; Accession no. 12805152) and a murine *prdx4* cDNA fragment (nt 257–576; Accession no. 7948998) were used as templates. Other templates were described previously (Frank et al., 1996; Madlener et al., 1998; Bloch et al., 2000; Hanselmann et al., 2001; Kumin et al., 2006).

Western blot and oxyblot analyses

Preparation of protein lysates and Western blot analysis were previously described (Kumin et al., 2006). A mouse monoclonal antibody against β-actin (Sigma-Aldrich) and a rabbit polyclonal antibody against Prdx6 (Kumin et al., 2006) were used. Oxidized proteins were detected using the OxyBlot assay kit (Chemicon) according to the manufacturer's instructions.

Immunofluorescence and immunohistochemistry

Sections were incubated overnight at 4°C with the primary antibodies diluted in PBS containing 3% BSA or 12% BSA and 0.025% NP-40. After three

washes with PBS/0.1% Tween 20, they were incubated for 1 h with the Cy2- or Cy3-conjugated secondary antibodies (Jackson ImmunoResearch Laboratories, Inc.), washed again and mounted with Mowiol (Hoechst). For immunohistochemistry biotinylated secondary antibodies (Jackson ImmunoResearch Laboratories, Inc.) were used, followed by counterstaining with hematoxylin. We used a mouse monoclonal antibody against α-SMA coupled to FITC (Sigma-Aldrich), rat monoclonal antibodies against MECA-32 or PECAM-1 (CD31) (both from BD PharMingen), a goat polyclonal antibody against pan-keratin (AbCam), and rabbit polyclonal antibodies against cleaved caspase-3 (Cell Signaling), fibrinogen/fibrin (DAKO), or nitrotyrosine (BIOMOL). For p53 immunohistochemistry PFA-fixed paraffin sections in combination with a polyclonal antibody against p53 (Novocastra) were used.

Light microscopy

Tissue sections were examined at room temperature by light microscopy using an Axioskop2 photomicroscope (Carl Zeiss, Inc.) and 10×/0.30, 20×/0.50, or 40×/1.30 Plan-Neofluar objectives (all from Carl Zeiss, Inc.). Images were acquired with an AxioCam HRc camera and AxioVision 4.1 software package set (Carl Zeiss, Inc.) and grouped with Adobe Photoshop or Illustrator (Adobe Systems).

Online supplemental material

The following information is available online as supplemental information: Fig. S1 shows a quantitative analysis of the wound healing process in Prdx6-deficient mice and wild-type controls, including the area of hyperproliferative wound epidermis, wound size, wound closure, and cell proliferation in the wound epidermis. Fig. S2 shows electron micrographs of wound vessels in Prdx6-deficient mice and control littermates at d 8 after injury. Fig. S3 demonstrates the successful generation of bone marrow chimeric mice as demonstrated by semi-quantitative and quantitative PCR for the Y-chromosome using DNA from blood and bone marrow cells. Fig. S4 shows electron micrographs of 7-d wounds of bone marrow-transplanted mice. Fig. S5 shows H/E stained sections from lung and skin of E13.5 Prdx6 embryos and wild-type littermates. Online supplemental material is available at http://www.jcb.org/cgi/content/full/jcb.200706090/DC1.

We thank Dr. Beverly Paigen (Jackson Laboratories, Bar Harbor, USA) for providing Prdx6 knockout mice and for helpful suggestions, Dr. Reinhard Dummer (University of Zurich) for help with the UVA experiments, Dr. Michael Detmar (ETH Zurich) for helpful suggestions with the quantification of blood vessels, Isabelle Planta-Wildenberg for help with the initial characterization of the knockout mice, and Anja Müller for help with the histology.

This work was supported by grants from the Swiss National Science Foundation (3100A0-109340/1), the ETH Zurich Research Foundation, the AETAS Foundation (to S.Werner), and the European Community (grant WOUND to S.Werner). M. Schäfer is a recipient of an EMBO postdoctoral fellowship.

Submitted: 13 June 2007
Accepted: 24 October 2007

References

Asahara, T., H. Masuda, T. Takahashi, C. Kalka, C. Pastore, M. Silver, M. Kearne, M. Magner, and J.M. Isner. 1999. Bone marrow origin of endothelial progenitor cells responsible for postnatal vasculogenesis in physiological and pathological neovascularization. *Circ. Res.* 85:221–228.

Ashcroft, G.S., and S.J. Mills. 2002. Androgen receptor-mediated inhibition of cutaneous wound healing. *J. Clin. Invest.* 110:615–624.

auf dem Keller, U., A. Kümin, S. Braun, and S. Werner. 2006. Reactive oxygen species and their detoxification in healing skin wounds. *J. Investig. Dermatol. Symp. Proc.* 11:106–111.

Bedard, K., and K.H. Krause. 2007. The NOX family of ROS-generating NADPH oxidases: physiology and pathophysiology. *Physiol. Rev.* 87:245–313.

Bloch, W., K. Huggel, T. Sasaki, R. Grose, P. Bugnon, K. Addicks, R. Timpl, and S. Werner. 2000. The angiogenesis inhibitor endostatin impairs blood vessel maturation during wound healing. *FASEB J.* 14:2373–2376.

Bluff, J.E., M.W.J. Ferguson, S. O'Kane, and G. Ireland. 2007. Bone marrow-derived endothelial progenitor cells do not contribute significantly to new vessels during incisional wound healing. *Exp. Hematol.* 35:500–506.

Braun, S., C. Hanselmann, M.G. Gassmann, U. auf dem Keller, C. Born-Berclaz, K. Chan, Y.W. Kan, and S. Werner. 2002. Nrf2 transcription factor, a novel target of keratinocyte growth factor action which regulates gene expression and inflammation in the healing skin wound. *Mol. Cell. Biol.* 22:5492–5505.

Cerutti, P.A., and B.F. Trump. 1991. Inflammation and oxidative stress in carcinogenesis. *Cancer Cells.* 3:1–7. Review.

Chang, H.Y., J.B. Sneddon, A.A. Alizadeh, R. Sood, R.B. West, K. Montgomery, J.T. Chi, M. van de Rijn, D. Botstein, and P.O. Brown. 2004. Gene expression signature of fibroblast serum response predicts human cancer progression: similarities between tumors and wounds. *PLoS Biol.* 2:E7.

Chen, J.W., C. Dodia, S.I. Feinstein, M.K. Jain, and A.B. Fisher. 2000. 1-Cys peroxiredoxin, a bifunctional enzyme with glutathione peroxidase and phospholipase A2 activities. *J. Biol. Chem.* 275:28421–28427.

Chomczynski, P., and N. Sacchi. 1987. Single-step method of RNA isolation by acid guanidinium thiocyanate-phenol-chloroform extraction. *Anal. Biochem.* 162:156–159.

Clark, R.A.F. 1996. Wound repair. Overview and general considerations. *In* The Molecular and Cellular Biology of Wound Repair. R.A.F. Clark, editor. Plenum Press, New York. 3–50.

Crosby, J.R., W.E. Kaminski, G. Schatteman, P.J. Martin, E.W. Raines, R.A. Seifert, and D.F. Bowen-Pope. 2000. Endothelial cells of hematopoietic origin make a significant contribution to adult blood vessel formation. *Circ. Res.* 87:728–730.

Darr, D., and I. Fridovich. 1994. Free-radicals in cutaneous biology. *J. Invest. Dermatol.* 102:671–675.

Frank, S., M. Madlener, and S. Werner. 1996. Transforming growth factors beta1, beta2, and beta3 and their receptors are differentially regulated during normal and impaired wound healing. *J. Biol. Chem.* 271:10188–10193.

Frank, S., B. Munz, and S. Werner. 1997. The human homologue of a bovine non-selenium glutathione peroxidase is a novel keratinocyte growth factor-regulated gene. *Oncogene.* 14:915–921.

Fujii, J., and Y. Ikeda. 2002. Advances in our understanding of peroxiredoxin, a multifunctional, mammalian redox protein. *Redox Rep.* 7:123–130.

Hanselmann, C., C. Mauch, and S. Werner. 2001. Haem oxygenase-1: a novel player in cutaneous wound repair and psoriasis? *Biochem. J.* 353:459–466.

Hawkins, B.J., M. Madesh, C.J. Kirkpatrick, and A.B. Fisher. 2007. Superoxide flux in endothelial cells via the chloride channel-3 mediates intracellular signaling. *Mol. Biol. Cell.* 18:2002–2012.

Hofmann, B., H.J. Hecht, and L. Flohe. 2002. Peroxiredoxins. *Biol. Chem.* 383:347–364.

Kumin, A., C. Huber, T. Rulicke, E. Wolf, and S. Werner. 2006. Peroxiredoxin 6 is a potent cytoprotective enzyme in the epidermis. *Am. J. Pathol.* 169:1194–1205.

Kunieda, T., M.W. Xian, E. Kobayashi, T. Imamichi, K. Moriwaki, and Y. Toyoda. 1992. Sexing of mouse preimplantation embryos by detection of Y-chromosome-specific sequences using polymerase chain-reaction. *Biol. Reprod.* 46:692–697.

Lee, T.H., S.U. Kim, S.L. Yu, S.H. Kim, D.S. Park, H.B. Moon, S.H. Dho, K.S. Kwon, H.J. Kwon, Y.H. Han, et al. 2003. Peroxiredoxin II is essential for sustaining life span of erythrocytes in mice. *Blood.* 101:5033–5038.

Madlener, M., W.C. Parks, and S. Werner. 1998. Matrix metalloproteinases (MMPs) and their physiological inhibitors (TIMPs) are differentially expressed during excisional skin wound repair. *Exp. Cell Res.* 242:201–210.

Manevich, Y., and A.B. Fisher. 2005. Peroxiredoxin 6, a 1-Cys peroxiredoxin, functions in antioxidant defense and lung phospholipid metabolism. *Free Radic. Biol. Med.* 38:1422–1432.

Manevich, Y., T. Sweitzer, J.H. Pak, S.I. Feinstein, V. Muzykantov, and A.B. Fisher. 2002. 1-Cys peroxiredoxin overexpression protects cells against phospholipid peroxidation-mediated membrane damage. *Proc. Natl. Acad. Sci. USA.* 99:11599–11604.

Manevich, Y., S.I. Feinstein, and A.B. Fisher. 2004. Activation of the antioxidant enzyme 1-CYS peroxiredoxin requires glutathionylation mediated by heterodimerization with pi GST. *Proc. Natl. Acad. Sci. USA.* 101:3780–3785.

Martin, P. 1997. Wound healing—aiming for perfect skin regeneration. *Science.* 276:75–81.

Mo, Y., S.I. Feinstein, Y. Manevich, Q. Zhang, L. Lu, Y.S. Ho, and A.B. Fisher. 2003. 1-Cys peroxiredoxin knock-out mice express mRNA but not protein for a highly related intronless gene. *FEBS Lett.* 555:192–198.

Monteiro, G., B.B. Horta, D.C. Pimenta, O. Augusto, and L.E.S. Netto. 2007. Reduction of 1-Cys peroxiredoxins by ascorbate changes the thiol-specific antioxidant paradigm, revealing another function of vitamin C. *Proc. Natl. Acad. Sci. USA.* 104:4886–4891.

Montesinos, M.C., J.P. Shaw, H. Yee, P. Shamamian, and B.N. Cronstein. 2004. Adenosine A(2A) receptor activation promotes wound neovascularization by stimulating angiogenesis and vasculogenesis. *Am. J. Pathol.* 164:1887–1892.

Munz, B., S. Frank, G. Hubner, E. Olsen, and S. Werner. 1997. A novel type of glutathione peroxidase: expression and regulation during wound repair. *Biochem. J.* 326:579–585.

Munz, B., M. Wiedmann, H. Lochmuller, and S. Werner. 1999. Cloning of novel injury-regulated genes. Implications for an important role of the muscle-specific protein skNAC in muscle repair. *J. Biol. Chem.* 274:13305–13310.

Nagy , N., G. Malik, A.B. Fisher, and D.K. Das. 2006. Targeted disruption of peroxiredoxin 6 gene renders the heart vulnerable to ischemia-reperfusion injury. *Am. J. Physiol. Heart Circ. Physiol.* 291:H2636–H2640.

Neumann, C.A., D.S. Krause, C.V. Carman, S. Das, D.P. Dubey, J.L. Abraham, R.T. Bronson, Y. Fujiwara, S.H. Orkin, and R.A. Van Etten. 2003. Essential role for the peroxiredoxin Prdx1 in erythrocyte antioxidant defence and tumour suppression. *Nature.* 424:561–565.

Pak, J. H., Y. Manevich, H.S. Kim, S.I. Feinstein, and A.B. Fisher. 2002. An antisense oligonucleotide to 1-cys peroxiredoxin causes lipid peroxidation and apoptosis in lung epithelial cells. *J. Biol. Chem.* 277:49927–49934.

Peshenko, I.V., and H. Shichi. 2001. Oxidation of active center cysteine of bovine 1-Cys peroxiredoxin to the cysteine sulfenic acid form by peroxide and peroxynitrite. *Free Radic. Biol. Med.* 31:292–303.

Rhee, S.G., S.W. Kang, T.S. Chang, W. Jeong, and K. Kim. 2001. Peroxiredoxin, a novel family of peroxidases. *IUBMB Life.* 52:35–41.

Sander, C.S., H. Chang, F. Hamm, P. Elsner, and J.J. Thiele. 2004. Role of oxidative stress and the antioxidant network in cutaneous carcinogenesis. *Int. J. Dermatol.* 43:326–335.

Steiling, H., B. Munz, S. Werner, and M. Brauchle. 1999. Different types of ROS-scavenging enzymes are expressed during cutaneous wound repair. *Exp. Cell Res.* 247:484–494.

Stuhlmeier, K.M., J.J. Kao, P. Wallbrandt, M. Lindberg, B. Hammarstrom, H. Broell, and B. Paigen. 2003. Antioxidant protein 2 prevents methemoglobin formation in erythrocyte hemolysates. *Eur. J. Biochem.* 270:334–341.

Tepper, O.M., J.M. Capla, R.D. Galiano, D.J. Ceradini, M.J. Callaghan, M.E. Kleinman, and G.C. Gurtner. 2005. Adult vasculogenesis occurs through in situ recruitment, proliferation, and tubulization of circulating bone marrow-derived cells. *Blood.* 105:1068–1077.

Thorey, I.S., J. Roth, J. Regenbogen, J.P. Halle, M. Bittner, T. Vogl, S. Kaesler, P. Bugnon, B. Reitmaier, S. Durka, et al. 2001. The Ca2+-binding proteins S100A8 and S100A9 are encoded by novel injury-regulated genes. *J. Biol. Chem.* 276:35818–35825.

Wang, L.J., Y.M. Chen, D. George, F. Smets, E.M. Sokal, E.G. Bremer, and H.E. Soriano. 2002. Engraftment assessment in human and mouse liver tissue after sex-mismatched liver cell transplantation by real-time quantitative PCR for Y chromosome sequences. *Liver Transpl.* 8:822–828.

Wang, X., S.A. Phelan, K. Forsman-Semb, E.F. Taylor, C. Petros, A. Brown, C.P. Lerner, and B. Paigen. 2003. Mice with targeted mutation of peroxiredoxin 6 develop normally but are susceptible to oxidative stress. *J. Biol. Chem.* 278:25179–25190.

Wang, Y., S.I. Feinstein, Y. Manevich, Y.S. Ho, and A.B. Fisher. 2004a. Lung injury and mortality with hyperoxia are increased in peroxiredoxin 6 gene-targeted mice. *Free Radic. Biol. Med.* 37:1736–1743.

Wang, Y., Y. Manevich, S.I. Feinstein, and A.B. Fisher. 2004b. Adenovirus-mediated transfer of the 1-cys peroxiredoxin gene to mouse lung protects against hyperoxic injury. *Am. J. Physiol. Lung Cell. Mol. Physiol.* 286:L1188–L1193.

Werner, S., W. Weinberg, X. Liao, K.G. Peters, M. Blessing, S.H. Yuspa, R.L. Weiner, and L.T. Williams. 1993. Targeted expression of a dominant-negative FGF receptor mutant in the epidermis of transgenic mice reveals a role of FGF in keratinocyte organization and differentiation. *EMBO J.* 12:2635–2643.

Werner, S., H. Smola, X. Liao, M.T. Longaker, T. Krieg, P.H. Hofschneider, and L.T. Williams. 1994. The function of KGF in morphogenesis of epithelium and reepithelialization of wounds. *Science.* 266:819–822.

Wood, Z.A., E. Schroder, J.R. Harris, and L.B. Poole. 2003. Structure, mechanism and regulation of peroxiredoxins. *Trends Biochem. Sci.* 28:32–40.

Yang, C.S., D.S. Lee, C.H. Song, S.J. An, S. Li, J.M. Kim, C.S. Kim, D.G. Yoo, B.H. Jeon, H.Y. Yang, et al. 2007. Roles of peroxiredoxin II in the regulation of proinflammatory responses to LPS and protection against endotoxin-induced lethal shock. *J. Exp. Med.* 204:583–594.